Journal of Geoscience and Environment Protection, 2026, 14(1), 159-182
https://www.scirp.org/journal/gep
ISSN Online: 2327-4344
ISSN Print: 2327-4336

Concurrent Impacts of ENSO and the Dipole Mode Index on Wet and Dry MAM Rainfall Variability in Zanzibar, Tanzania (1981-2024)

Mohammed Yussuf Bakar[1,2*], Zhao Yu[1], Daudi Ndabagenga[1,2], Madundo Albert[1,2], Mhenzi Fredy[1,2], Silla Abdoul[1], Msafiri Mtupili[2], Miraji Khamis[2]

[1]School of Atmospheric Sciences, Key Laboratory of Meteorological Disaster of the Ministry of Education, Nanjing University of Information Science and Technology, Nanjing, China
[2]Tanzania Meteorological Authority (TMA), Dodoma, Tanzania
Email: *mobakar078@gmail.com

How to cite this paper: Bakar, M. Y., Yu, Z., Ndabagenga, D., Albert, M., Fredy, M., Abdoul, S., Mtupili, M., & Khamis, M. (2026). Concurrent Impacts of ENSO and the Dipole Mode Index on Wet and Dry MAM Rainfall Variability in Zanzibar, Tanzania (1981-2024). *Journal of Geoscience and Environment Protection, 14,* 159-182.
https://doi.org/10.4236/gep.2026.141010

Received: December 20, 2025
Accepted: January 19, 2026
Published: January 22, 2026

Copyright © 2026 by author(s) and Scientific Research Publishing Inc.
This work is licensed under the Creative Commons Attribution International License (CC BY 4.0).
http://creativecommons.org/licenses/by/4.0/
Open Access

Abstract

This study investigates the concurrent impacts of the El Niño-Southern Oscillation (ENSO) and the Indian Ocean Dipole (IOD), represented by the Dipole Mode Index (DMI), on March-April-May (MAM) rainfall variability in Zanzibar, Tanzania, during the period 1981-2024. Analysis of Empirical Orthogonal Function (EOF), Concurrent ENSO-DMI phases and atmospheric circulations of wet and dry years during the study period were examined. The results reveal that the first leading mode (EOF1) of rainfall variability accounts for 88% of the total variance and exhibits a spatially coherent pattern across both Unguja and Pemba islands. The associated principal component (PC1) exhibits a strong positive spatial correlation with sea surface temperature anomalies in the Niño 3.4 region (r = 0.7) and a weak positive spatial correlation within the DMI region (r = 0.3), indicating the influence of both the tropical Pacific and Indian Oceans on seasonal rainfall variability. Further analysis of the concurrent ENSO-DMI impacts on wet and dry years shows that, during wet MAM seasons, the concurrent frequency of El Niño and positive IOD phases dominates at 50%, while La Niña and positive IOD co-occur in 33.3%. In contrast, dry years are largely dominated by the concurrence of La Niña and positive IOD, accounting for 71.5% of dry events, which exceeds the contribution from La Niña combined with negative IOD (28.5%). Further analysis of composite atmospheric circulation analyses indicate that enhanced rainfall is linked to low-level cyclonic circulation, moisture convergence, and upward motion. In contrast, the dry conditions correspond to anticyclonic flow, moisture divergence, and subsidence. These findings demonstrate that MAM rainfall variability in Zanzibar is more modulated more by El Niño-positive IOD (La Niña-positive

IOD) phases during wet (dry) years, together with regional atmospheric dynamics, underscoring the importance of considering multiple climate drivers for improved seasonal forecasting and climate adaptation planning.

Keywords

MAM Rainfall, ENSO, Indian Ocean Dipole, Climate Variability, Zanzibar

1. Introduction

The Zanzibar Archipelago, located off the eastern coast of Tanzania, relies heavily on the March-April-May (MAM) rainy season as its primary source of freshwater for domestic use, agriculture, and ecosystem sustainability (Chabaga et al., 2025; Greene et al., 2020; TMA, 2025). Despite its importance, MAM rainfall over Zanzibar exhibits pronounced interannual variability, with recurrent episodes of drought and flooding that undermine food security, water resource management, and socio-economic stability (Greene et al., 2020; Ndabagenga et al., 2023; TMA, 2022). These vulnerabilities are expected to intensify under ongoing climate variability and change, making a robust understanding of the dynamical drivers of MAM rainfall a critical prerequisite for effective weather forecasting, climate adaptation, and risk reduction in the region (IPCC, 2023; Magang et al., 2024; IPCC, 2018; WMO, 2015).

Interannual rainfall variability across East Africa is largely influenced by major large-scale ocean-atmosphere coupled systems, particularly ENSO, the IOD, the Madden-Julian Oscillation (MJO), and the Quasi-Biennial Oscillation (QBO) (Assenga & Ndabagenga, 2025; Gudoshava et al., 2024; Nicholson, 2017; Palmer et al., 2023). Over mainland Tanzania, numerous studies have shown that El Niño events generally enhance rainfall during the October-November period (Mbigi & Xiao, 2021; Ntigwaza & Wang, 2024; Rwambo et al., 2025) and contribute to increased precipitation during the MAM season (Kebacho & Chen, 2022; Rwambo et al., 2025). For example, (King'uza & Tilwebwa, 2019), in their study on the interannual variability of March-May rainfall in Tanzania, reported strong positive correlations between the Niño 3.4 and Tropical North Atlantic (TNA) indices and MAM rainfall along the country's eastern coastal region. Regardless of the impacts of ENSO and the IOD, other studies have also investigated the role of atmospheric circulation in modulating MAM rainfall variability over Tanzania, including the Zanzibar domain (Kebacho, 2022; Kebacho & Chen, 2022; King'uza & Tilwebwa, 2019; Mafuru & Guirong, 2018). For instance, most studies concur that enhanced low-level moisture flux convergence, lower geopotential heights, reduced outgoing longwave radiation (OLR), and increased accumulation of water vapor over the region favor cyclonic circulation, increased cloudiness, and enhanced convective activity, thereby reinforcing rainfall development (Kebacho & Chen, 2022;

Makula & Zhou, 2021). Conversely, moisture divergence, higher geopotential heights, increased OLR, and reduced humidity suppress convection and lead to below-normal MAM rainfall (Borhara et al., 2020; Chabaga et al., 2025; King'uza & Tilwebwa, 2019).

Moreover, different studies have been conducted over the Zanzibar domain (Finney et al., 2021; Kai et al., 2021b) with some even examining the impacts of tropical cyclones on MAM rainfall variability in Zanzibar. For example, a noteworthy study by (Kai et al., 2021a) documented anomalous rainfall characteristics in Zanzibar during Tropical Cyclone Fantala in 2016, where 16-day accumulated rainfall totals ranged from 551 mm at Kizimbani to 256 mm at Matangatuani. In addition to tropical cyclone, this underscores the importance of examining Zanzibar's rainfall variability in relation to large-scale teleconnection patterns such as ENSO and IOD dynamics. Additionally, diurnal precipitation variability on tropical islands like Zanzibar has been reported to be shaped by sea-land breeze circulations driven by differential land-ocean heating and local orographic influences (Camberlin, 2018; Zhu et al., 2017).

Although various studies on ENSO and IOD impacts have been conducted over the study domain and their impacts are well known, there remains a need to investigate the concurrent effects of ENSO and IOD (DMI) on MAM rainfall variability over the region. As explained above in the literature, most existing studies have focused on the impacts of ENSO and IOD individually, particularly how they influence enhanced or reduced rainfall over the study domain, without explaining the frequency of their concurrent phases. This leaves several challenging questions unanswered. For example: Which concurrent ENSO-DMI phases predominantly affect Zanzibar's MAM rainfall variability? Which concurrent ENSO-DMI phases dominate over others? To what extent do the dominant concurrent ENSO-DMI phases influence the wet and dry years of MAM rainfall variability over Zanzibar? This study directly addresses these gaps. Understanding the concurrent effects is crucial, as combined climate modes often exert a stronger influence on regional climate than either mode acting alone (Endris et al., 2019; Nguyen-Le et al., 2024; Sarkar et al., 2024). Such understanding also improves the predictability of wet and dry seasons, enhances early warning capabilities for climate-related hazards, and provides valuable insights for climate risk management, agricultural planning, and water resource decision-making over the study domain. In this study, we first apply EOF analysis to characterize MAM rainfall variability in Zanzibar. Second, we use Pearson's correlation analysis to examine the relationship between MAM rainfall variability and global sea surface temperature. We then advance by investigating the concurrent impacts of ENSO-DMI phases on wet and dry years during the MAM rainfall season. Finally, we investigate the influence of atmospheric circulations on wet and dry years of MAM rainfall season. The remainder of the paper is organized as follows: Section 2 describes the data and methodology, Section 3 presents the results, Section 4 discusses the findings, and Section 5 provides the conclusions.

2. Data and Methodology

2.1. Study Area

Zanzibar comprises two main islands, Unguja and Pemba (**Figure 1**), located in the southwestern Indian Ocean, approximately 35 km and 56 km off the East African coast, respectively. Geographically, Unguja spans 5.75˚S - 6.5˚S and 39.27˚E - 39.53˚E, while Pemba lies between 4.93˚S - 5.28˚S and 39.67˚E - 39.73˚E (Abdalla et al., 2023; Bakari et al., 2023). The islands are generally low-lying, with elevations ranging from sea level along the coasts to about 300 m in the central and western highlands of Unguja. Pemba is slightly more undulating, with maximum elevations reaching 250 m. Zanzibar experiences a tropical bimodal rainfall regime, characterized by two distinct wet seasons, the long rains (Masika) from March to May (MAM) and the short rains (Vuli) from October to December (OND) (Kijazi & Reason, 2009; Suleiman et al., 2023). The MAM season is the climatologically dominant rainy period, marked by abundant rainfall with strong temporal and spatial coherence across both islands (Kai et al., 2021b). In contrast, the OND season exhibits weaker, more erratic rainfall with limited spatial coverage (Assenga et al., 2025). These rainfall patterns are driven by seasonal shifts in monsoon circulation. The MAM rains are primarily influenced by southeasterly to southwesterly monsoon flows that advect moisture from the Indian Ocean, while the OND rains are associated with the northeast monsoon (Kebacho, 2022). During MAM, the long-term average maximum temperatures range from 32.4˚C (Unguja) to 31.6˚C (Pemba), with minima of 22.7˚C and 23.1˚C, respectively (TMA, 2022). The key socio-economic activities underpinning Zanzibar's annual GDP include small-scale agriculture, tourism, commerce, and fisheries, supplemented by sand mining and emerging blue-economy sectors (Abdalla et al., 2023; Greene et al., 2020).

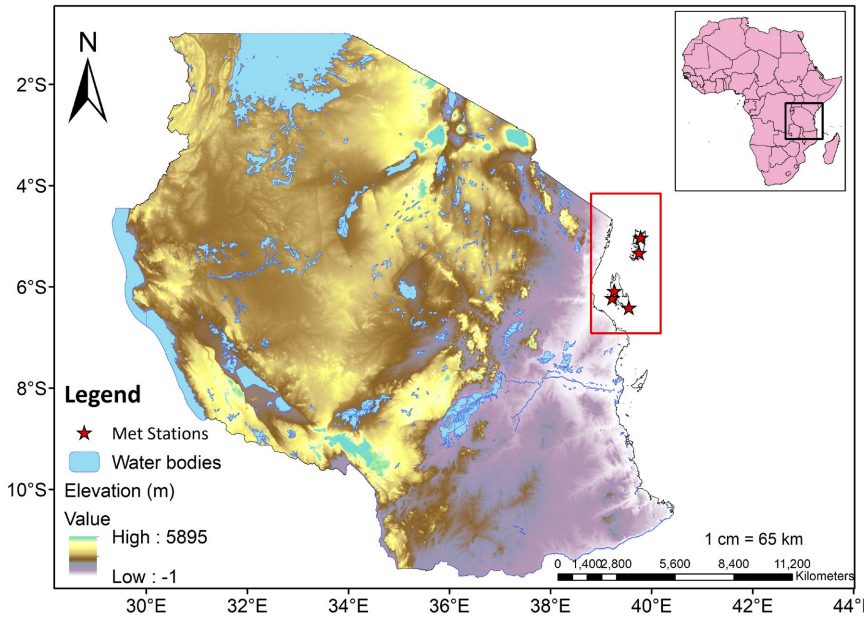

Figure 1. Map of Tanzania, showing the study area, Zanzibar islands (Unguja and Pemba) in the red solid box, with the distribution of meteorological stations (red stars).

2.2. Data Sources

This study integrates satellite-based precipitation data, atmospheric reanalysis, and ground-based observations to analyze MAM rainfall variability over Zanzibar from 1981 to 2024. The primary rainfall dataset is the Climate Hazards Group InfraRed Precipitation with Stations (CHIRPS) version 2.0, which provides daily precipitation estimates at a 0.05˚ × 0.05˚ (~5 km) spatial resolution across the global tropics (50˚S - 50˚N) for the period 1981-2024. CHIRPS combines thermal infrared satellite imagery, a high-resolution climatology (CHPclim), and in-situ rain gauge data to produce a consistent, bias-corrected product that has been extensively validate across East Africa (EA) for monitoring droughts and climate trends (Dinku et al., 2018; Funk et al., 2015; Ndabagenga et al., 2023). The dataset is publicly available at https://data.chc.ucsb.edu/products/CHIRPS-2.0/.

To diagnose the atmospheric drivers of rainfall variability, ERA5 reanalysis data from the European Centre for Medium-Range Weather Forecasts (ECMWF) were used for the same period (Hersbach et al., 2020). ERA5 provides global atmospheric variables at a high horizontal resolution of 0.25˚ × 0.25˚, making it well-suited for regional climate diagnostics in the western Indian. Key variables include sea surface temperature (SST), geopotential height, vertical velocity (omega, in Pa/s), zonal (u) and meridional (v) wind components, and specific humidity at multiple pressure levels. These fields enabled the computation of moisture flux divergence (MFD), vertical motion composites, and wind anomaly patterns to assess the influence of large-scale climate models, particularly ENSO and DMI, on Zanzibar's MAM rainfall. ERA5 data were accessed via the Copernicus Climate Data Store and is openly available at https://cds.climate.copernicus.eu/.

For validation, daily rainfall observation data from six synoptic stations operated by the Tanzania Meteorological Authority (TMA) were used: Kilombero, Kizimbani, Makunduchi, Pemba Airport, Wete, and Zanzibar Airport (**Figure 1**). Monthly aggregated data from 2015 to 2024 were compared with corresponding CHIRPS estimates to evaluate spatial representativeness and temporal fidelity. This ground-truthing step ensures that satellite-derived anomalies accurately reflect local rainfall behavior.

2.3. Methodology

2.3.1. Validation of CHIRPS Rainfall Data

The Climate Hazards Group InfraRed Precipitation with Station data (CHIRPS) is validated against ground-based station observations to ensure its reliability for climatological analysis across the study region as shown in **Figure 2**. The validation was accomplished through the Statistical Correlation Analysis, in which the Scatter plots of monthly precipitation values from January 2015 to December 2024 are generated for each station. The Pearson correlation coefficient (r) is calculated to quantify the linear relationship between the satellite estimates and ground observations. A strong positive linear relationship is detected between CHIRPS estimates and ground observations, with Correlation coefficients (r) ranging from 0.83 (Wete) to 0.93 (Kizimbani), indicating high reliability of the CHIRPS dataset

for climatological studies across the study area. This performance of CHIRPS aligns with previous findings (Dinku et al., 2018).

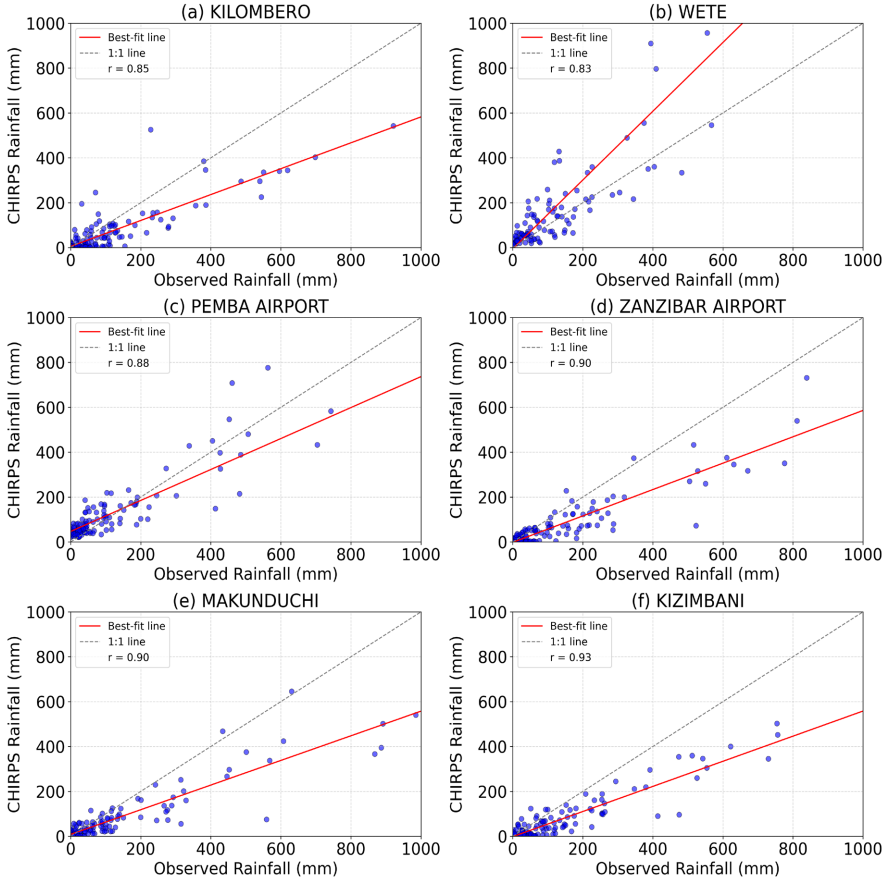

Figure 2. Correlation analysis between CHIRPS rainfall estimates and ground observations (mm) for six locations: (a) Kilombero, (b) Wete, (c) Pemba airport, (d) Zanzibar airport, (e) Makunduchi. and (f) Kizimbani. The magnitude of the relationship is shown by the correlation coefficient (r), and a solid red line shows the direction of the correlation.

2.3.2. Analysis of Dominant Rainfall Variability Modes during MAM Season Equations

The dominant modes of MAM rainfall variability were identified using Empirical Orthogonal Function analysis applied to the CHIRPS rainfall field over Zanzibar (1981-2024). EOF decomposes the spatiotemporal dataset into orthogonal spatial patterns and their associated temporal coefficients, known as principal components (PCs). The first mode and its time series explain the majority of total variance and were used to define wet and dry years for composite analysis. All values of PC1 ≥ 1 were considered as wet years while those ≤1 were considered as dry years. The EOF method has also been used by many other different studies over the study domain (Kebacho & Chen, 2022; King'uza & Tilwebwa, 2019; Suleiman et al., 2023). The results of wet and dry years computed from PC1 were used in the analysis of concurrent impacts of ENSO and DMI phases on MAM rainfall variability in Zanzibar for the study period.

2.3.3. Determination of Dominant Frequency of Concurrent ENSO and DMI Phases

Following the identification wet and dry years from PC1 of MAM rainfall over the study domain, the two dominant climate modes, ENSO and DMI were assessed during these years. The Niño3.4 index was computed as the area-averaged SSTA over the equatorial Pacific region (5˚S - 5˚N, 170˚W - 120˚W); positive/negative values signify El Niño/La Niña conditions while zero value indicates neutral condition. The DMI was calculated as the difference in SSTA between the western Indian Ocean (10˚S - 10˚N, 50˚E - 70˚E) and the eastern Indian Ocean (10˚S - 0˚, 90˚E - 110˚E), with positive (negative) values indicating positive (negative) IOD phases. The definitions and regional boundaries of Niño3.4 and DMI can be found in (Yu & Kim, 2013). Subsequently, the dominant concurrent frequencies (D.F) of ENSO and IOD phases during anomalously wet and dry MAM years were quantified using the following equations;

$$\%\mathrm{D.F}_{\text{wet years}} = \frac{\text{Number of ENSO/DMI phases}}{\text{Total ENSO/DMI phases of wet years}} \times 100 \quad (1)$$

$$\%\mathrm{D.F}_{\text{dry years}} = \frac{\text{Number of ENSO/DMI phases}}{\text{Total ENSO/DMI phases of wet years}} \times 100 \quad (2)$$

2.3.4. Correlation Coefficient Method

The Pearson's correlation coefficient was used in different stages of this research (Hauke & Kossowski, 2011). First, it was used in the validation of CHIRPS data against ground-based station observations to ensure its reliability for climatological analysis across the study, as explained in section 2.3.1. Also, it was used to assess both spatial and long-term temporal correlation between MAM rainfall PCs and SSTA. At this stage, Pearson's correlation coefficient was computed between PC1 and PC2 and gridded global SSTA to evaluate the influence of sea surface temperatures in the central Pacific Ocean, as well as the western and eastern Indian Ocean, on MAM rainfall variability over the study domain. The Peason's correlation coefficient (r) is given by;

$$r_{xy} = \frac{\sum_{i=1}^{n}(x_i - \bar{x})(y_i - \bar{y})}{\sum_{i=1}^{n}(x_i - \bar{x})^2 \cdot \sum_{i=1}^{n}(y_i - \bar{y})^2} \quad (3)$$

where x_i and y_i denote MAM rainfall PCs and SSTA, respectively, and $\bar{x}$ and $\bar{y}$ represent their mean values.

2.3.5. Trend and Statistical Significance Testing

To assess whether the relationship between the MAM rainfall PCs and global sea surface temperature (SST) anomalies is statistically significant, a student's t-test was applied to the Pearson correlation coefficients at each grid point. This test evaluates whether the observed correlation is significantly different from zero, assuming approximate normality and independence of the time series. The t-statistic is computed as;

$$t = r\sqrt{\frac{n-2}{1-r^2}} \quad (4)$$

where r is the Pearson correlation coefficient between the PC and SST time series, n is the number of temporal samples (years), and $n-2$ represents the degrees of freedom. Finally, the Student t-test was used to quantify the significance between PCs and the global SST at 99% confidence level.

2.3.6. Composite Anomaly Computation in Atmospheric Circulations

Finally, the results of wet and dry years were investigated together with atmospheric circulation variables, including relative humidity, geopotential height, omega, wind, and moisture divergence flux, to diagnose the large-scale ocean-atmosphere drivers of Zanzibar's rainfall extremes. For each variable, the MAM-mean was calculated for every year (1981-2024). Composites for the wettest and driest years were then computed as:

$$\text{Composite}_{\text{wet}} = \frac{1}{5}\sum_{i=1}^{5} X_{\text{wet},i} \tag{5}$$

$$\text{Composite}_{\text{dry}} = \frac{1}{5}\sum_{i=1}^{5} X_{\text{dry},i} \tag{6}$$

where X denotes the MAM-mean field of a given variable in year i.

To highlight deviations from the long-term norm, anomalies were derived by subtracting the 1981-2024 climatological mean ($\overline{X}_{\text{clim}}$) from each composite as follows:

$$\text{Anomaly}_{\text{wet}} = \text{Composite}_{\text{wet}} - \overline{X}_{\text{clim}} \tag{7}$$

$$\text{Anomaly}_{\text{dry}} = \text{Composite}_{\text{dry}} - \overline{X}_{\text{clim}} \tag{8}$$

Finally, the difference between wet and dry composites was computed as:

$$\text{Difference} = \text{Composite}_{\text{wet}} - \text{Composite}_{\text{dry}} \tag{9}$$

3. Results

3.1. Rainfall Variability during MAM Season in Zanzibar (1981-2024)

3.1.1. Climatology of Rainfall during MAM Season

To observe rainfall variability in Zanzibar, first, the Climatology was analyzed as shown in **Figure 3**. The results show that during MAM season rainfall begins modestly in March with amount of rainfall <200 mm across most areas (**Figure 3(a)**), intensifies sharply in April, peaking at over 500 mm on Pemba Island and some parts of northern Unguja (**Figure 3(b)**), and declines in May (**Figure 3(c)**), especially over southern Unguja, which receives less than 100 mm. This progression underscores April as the core wet month of the season, aligning with the broader East African (EA) rainfall regime. Spatially, a pronounced north-south gradient dominates the MAM rainfall distribution across the archipelago (**Figure 3(d)**). Pemba Island consistently records the highest seasonal totals (400 - 600 mm), while northern Unguja receives moderate rainfall (300 - 400 mm), and southern Unguja remains relatively dry (<200 mm). This heterogeneity likely arises from a combination of topographic effects, such as orographic enhancement on Pemba's

elevated terrain, and regional atmospheric circulation patterns that favor moisture convergence in the northern islands.

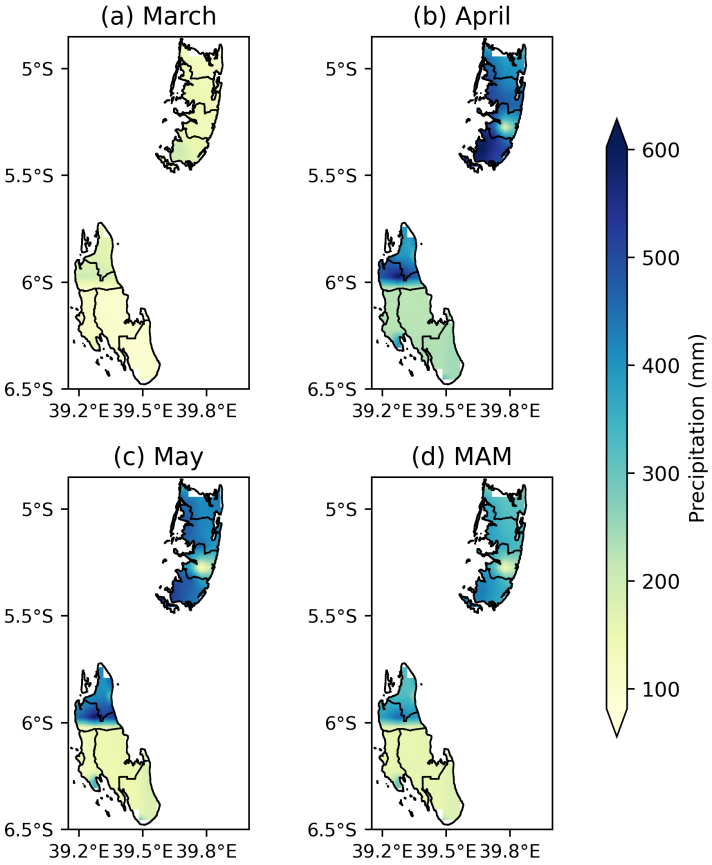

Figure 3. Zanzibar MAM (March-April-May) rainfall climatology (1981-2024). Spatial distribution of mean monthly precipitation (mm) for (a) March, (b) April, (c) May, and (d) the full MAM season.

3.1.2. MAM Seasonal Rainfall Anomaly across Zanzibar

Second, analysis of standardized precipitation anomalies during the MAM season was carried out to provide insights into both spatial and temporal variability of rainfall across Unguja and Pemba islands as shown in **Figure 4**. The results in the spatial map indicate consistent positive rainfall anomalies across both Unguja and Pemba Islands, with values ranging from +0.5 to +1.5 units (**Figure 4(a)**), suggesting a general tendency toward above-average rainfall during this season over the 44 years. This pattern indicates that Zanzibar's MAM rainfall is more frequently above normal than below, which may reflect regional climatic stability or a long-term shift in moisture availability. The uniformity of the anomaly field, with no strong negative patches, implies that dry spells are less spatially extensive than wet events. In (**Figure 4(b)**), interannual variability is pronounced, with extreme wet years such as 1986, 2017, 2018, 2019, and 2020 standing out (green dots > +1), while dry years like 2003, 2009, 2011, 2012, and 2022 (red dots < −1) are less frequent but still impactful.

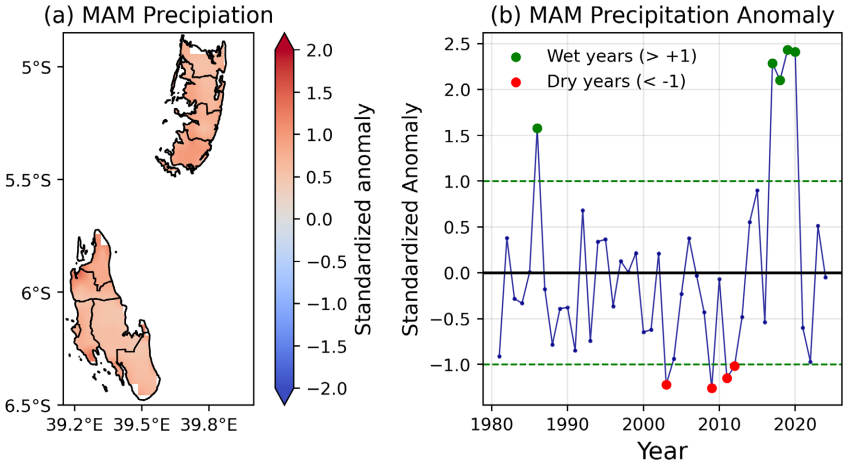

Figure 4. MAM (March-April-May) standardized precipitation anomalies over Zanzibar (1981-2024). (a) The spatial pattern of area-averaged standardized anomalies, showing dominant positive anomalies (red) across both Unguja and Pemba Islands. (b) The time series of annual MAM standardized anomalies (blue line), with wet years (>+1) marked in green and dry years (<−1) in red.

3.1.3. Dominant Mode of MAM Seasonal Rainfall Variability

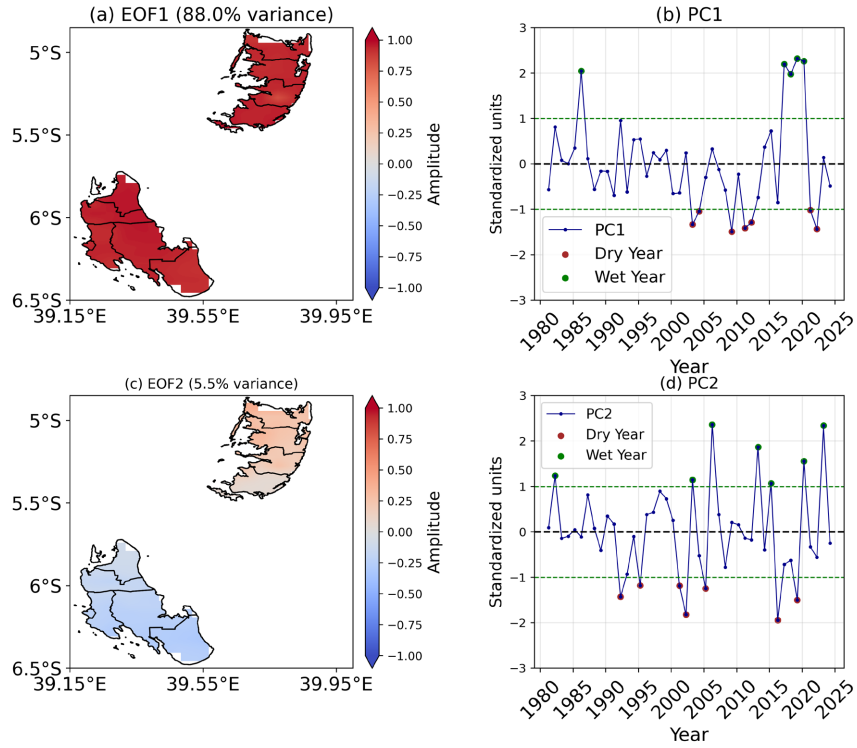

Figure 5. Empirical Orthogonal Function (EOF) analysis of MAM (March-April-May) rainfall over Zanzibar for the period 1981-2024. (a) The first EOF mode (EOF1), explaining 88.0% of the total variance, exhibits a uniform positive spatial pattern across both Unguja and Pemba Islands. (b) The corresponding Principal Component time series (PC1), with wet years (>+1) indicated in green and dry years (<−1) in red. (c) and (d) show the second EOF mode (EOF2) and its associated Principal Component (PC2), respectively.

Finally, the investigation was extended to the EOF analysis of MAM precipitation anomalies over Zanzibar for the period 1981-2024 as indicated in Figure 5. The results reveal the dominant spatial and temporal modes governing seasonal rainfall variability. Collectively, the first EOF mode accounting for 88.0% of total variance, reveals a spatially coherent pattern of MAM rainfall anomalies across Zanzibar, with positive loadings dominating both Unguja and Pemba Islands (Figure 5(a)). The associated time series PC1 captures this dominant signal, with notable wet extremes in 1986, 1992, 2017, 2018, 2019, and 2020, and dry extremes in 2003, 2004, 2009, 2011, 2012, 2021, and 2022 (Figure 5(b)).

The second EOF mode (Figure 5(c)), explaining 5.5% variance, exhibits a north-south dipole structure of positive anomalies in Pemba and negative anomalies in Unguja. This highlights that in secondary mode, rainfall variability is out-of-phase between the islands in Zanzibar. The PC2 time series in Figure 5(d) shows more erratic behavior, with no clear trend, reinforcing that this mode represents regional-scale noise or modulation rather than a basin-wide driver. Due to this reason, the wet and dry years from MAM PC1 were selected and subsequently used to assess concurrent impacts of ENSO-DMI phases as well as the impacts of atmospheric circulations Zanzibar MAM rainfall variability.

3.2. Effects of Global Sea Surface Temperature (SST) on MAM Rainfall Variability 1981-2024

In this section, both the long-term spatial and temporal correlation between Global SST and PCs of MAM rainfall variability in Zanzibar were investigated for the study period 1981-2024 as shown in Figure 6.

PC1 exhibits a strong positive correlation (r = 0.7) with SST anomalies in the central-eastern tropical Pacific (NINO3.4 region) (Figure 6(a)). In contrast, PC2 reveals a weaker but spatially distinct relationship, with negative correlation (r = -0.3) over the central equatorial Pacific (Figure 6(b)). On the other hand, PC1 shows spatial weak positive correlation (r = 0.3) within the DMI regions while PC2 shows weak positive correlation (r = 0.3) over DMI west pole and negative weak correlation over east pole. The investigation was also extended to analyze global SST anomalies during wet and dry years as shown in Figure 7. The results indicate wet (dry) years are associated with above (below) normal SST anomalies, and above normal SST anomalies for wet minus dry years Figures 7(a)-(c).

The investigation was also extended to analyze global SST anomalies during wet and dry years as shown in Figure 7. The results indicate wet/dry years are associated with above/below normal SST anomalies, and above normal SST anomalies for wet minus dry years Figures 7(a)-(c).

Moreover, the temporal variability of PCs MAM rainfall, ENSO and DMI were analyzed as indicated in Figure 8(a), Figure 8(b). The PC1 during MAM is out of phase with ENSO in some years (La Niña occurring during wet years or El Niño during dry years), and similarly out of phase with the DMI (negative IOD during wet years or positive IOD during dry years). As a result, the PC1 shows only a weak positive correlation (r = 0.3) with both ENSO and the DMI.

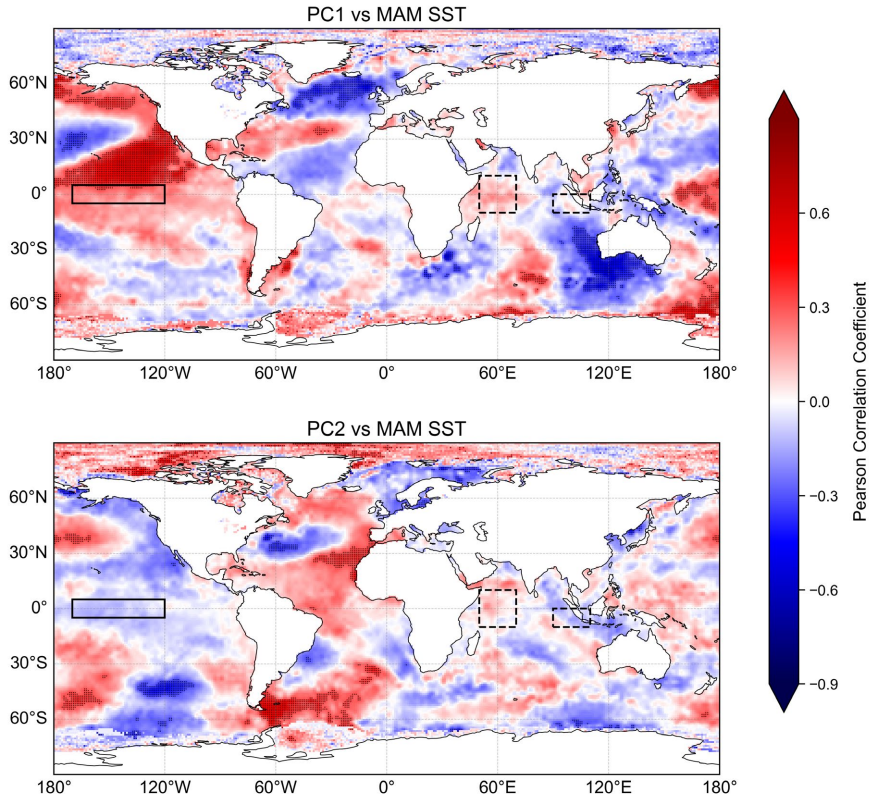

Figure 6. Correlation coefficients between (a) MAM rainfall PC1 and (b) PC2 and global MAM sea surface temperature anomalies over 1981-2024. The black boxes indicate the Niño3.4 region (5˚S - 5˚N, 170˚W - 120˚W) in the central equatorial Pacific, the Dipole Mode Index region in the western Indian Ocean (10˚S - 10˚N, 50˚E - 70˚E), and the eastern Indian Ocean (10˚S - 0˚, 90˚E - 110˚E), respectively. Hatched areas denote correlations that are statistically significant at the 99% confidence level, based on a student's t-test.

3.3. Concurrence of ENSO and DMI during Wet and Dry Years of MAM Rainfall in Zanzibar

The concurrence assessment of ENSO-DMI phases during MAM rainfall was analyzed for the period 1981-2024, and are shown in Table 1. The results reveal that some wet years (e.g., 1986 and 2018) coincided with La Niña events combined with positive IOD phases, whereas others (2015, 2019, and 2020) occurred during El Niño events coupled with positive IOD phases. A key outcome of this analysis is that most wet years are associated with positive IOD phases, highlighting its dominant role in enhancing MAM rainfall over Zanzibar. Moreover, the concurrence of El Niño and positive IOD accounts for 50% of the wet years, whereas the concurrence of La Niña and positive IOD contributes 33.3% while El Niño and negative IOD co-occur by 16.7% (Table 2). This indicates that although both ENSO phases can produce wet conditions when accompanied by most positive IOD, the El Niño-positive IOD combination exerts a stronger influence on MAM rainfall enhancement. Also, a similar analysis of the dry years shows that most dry years coincided with La Niña events together with positive IOD phases, while 2012 and 2022 occurred during La Niña combined with negative IOD phases. These

results demonstrate that La Niña conditions dominate all dry years, underscoring its strong suppressing effect on MAM rainfall over Zanzibar. Additionally, the concurrence of La Niña and positive IOD accounts for 71.5% of the dry years, while the concurrence of La Niña and negative IOD and El Niño with negative IOD collectively accounts for 28.5%. This suggests that even when the IOD is in a positive phase, La Niña can still exert a controlling influence leading to suppressed rainfall. However, there is still statistical limitations associated with the small sample sizes used in Table 2. The percentages reflect the relative frequency of specific historical concurrent ENSO-IOD occurrences during the study period (1981-2024), rather than robust climatological probabilities.

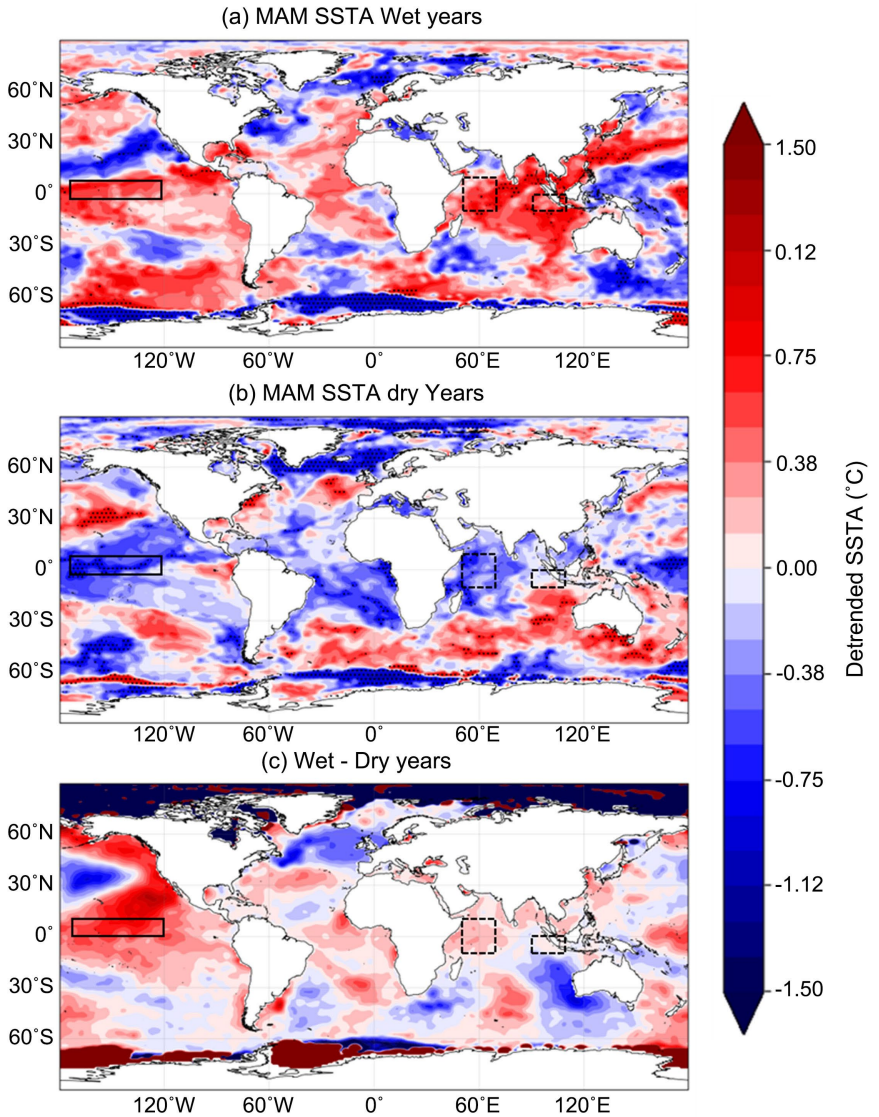

Figure 7. Composite MAM sea surface temperature anomalies (˚C) for (a) wet years, (b) dry years, and (c) wet-minus-dry differences. The black boxes represent the Niño3.4 region (5˚S - 5˚N, 170˚W - 120˚W) over the central equatorial Pacific, the Dipole Mode Index region in the western Indian Ocean (10˚S - 10˚N, 50˚E - 70˚E), and the eastern Indian Ocean (10˚S - 0˚, 90˚E - 110˚E), respectively.

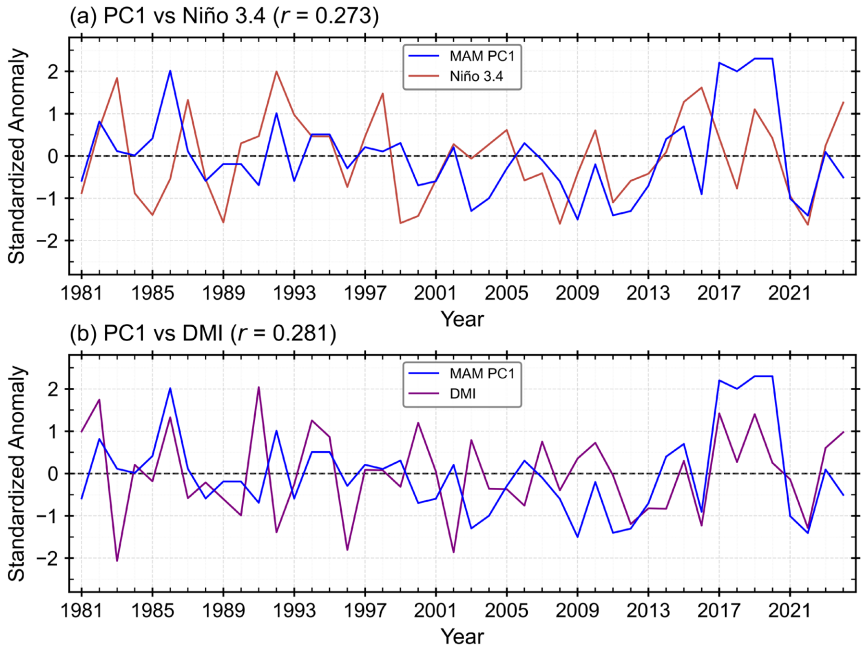

Figure 8. Longterm temporal correlation between Zanzibar MAM rainfall PCs and Nino3.4 index and DMI 1981-2024.

Table 1. Concurrent ENSO-DMI phases of MAM rainfall in Zanzibar for the period 1981-2024.

Wet years (MAM)			Dry years (MAM)		
Years	El Niño / La Niña	pIOD/ nIOD	Years	El Niño / La Niña	pIOD/ nIOD
1986	La Niña	pIOD	2003	La Niña	pIOD
1992	El Niño	nIOD	2004	La Niña	pIOD
2017	El Niño	pIOD	2009	La Niña	pIOD
2018	La Niña	pIOD	2011	La Niña	pIOD
2019	El Niño	pIOD	2012	La Niña	nIOD
2020	El Niño	pIOD	2021	La Niña	pIOD
	-	-	2022	La Niña	nIOD

pIOD = positive IOD phase, nIOD = negative IOD phase.

Table 2. The frequency of concurrent ENSO-DMI phases of MAM rainfall in Zanzibar for the period 1981-2024.

Wet years (MAM)			Dry years (MAM)		
Concurrent phases	No.	Frequency (%)	Concurrent phases	No.	Frequency (%))
La Niña /pIOD	2	33.3	La Niña /pIOD	5	71.5
El Niño /nIOD	1	16.7	La Niña /nIOD	2	28.5
El Niño /pIOD	3	50.0	-		

3.4. Atmospheric Circulations

3.4.1. Effects of Relative Humidity and Wind Anomalies during Wet and Dry Years of MAM Rainfall

The composite analysis of RH and wind anomalies shown in Figure 9 highlights atmospheric circulation patterns over the Zanzibar Islands (the black box) during the wet and dry MAM season for the study period. The investigation reveals that during wet years indicated in Figure 9(a), the lower troposphere (850 hPa) exhibits pronounced positive relative humidity (RH) anomalies ranging between 2.5% - 7.0%, indicating enhanced moisture availability. This is accompanied by anomalous low-level winds converging on the region from the Indian Ocean, particularly from the southeast, facilitating robust moisture advection into Zanzibar. The high relative humidity anomalies depicted in Figure 9(a) still persist in Figure 9(b) at upper levels (250 hPa), showing that wet years are characterized by elevated RH and strong easterly and northeasterly flow, suggesting active deep convection and efficient upper-level divergence, which are the key ingredients for enhanced rainfall. In contrast, dry MAM years show widespread negative RH anomalies at both levels ranging −2.5% - 5.0% (Figure 9(c) and Figure 9(d)), with divergent or weak low-level flow and suppressed upper-level outflow, reflecting atmospheric drying and inhibited convection. The composite difference (Figure 9(e) and Figure 9(f)) still indicates positive relative anomalies above normal highlighting that Zanzibar's rainfall variability is dynamically driven by large-scale moisture convergence and vertical motion patterns, with the strongest signal localized within the black box region encompassing the islands.

3.4.2. The Influences of Wind and Geopotential Height Anomalies during Wet and Dry Years

The composite GPH anomalies and associated wind patterns over Zanzibar during wet and dry MAM seasons highlight the synoptic-scale circulation differences influencing MAM rainfall (Figure 10). During wet MAM seasons over Zanzibar (the black box), the lower troposphere (Figure 10(a)) exhibits a pronounced negative anomaly, indicating lower pressure and enhanced cyclonic circulation, which favors upward motion and rainfall. This pattern is accompanied by the Indian Ocean southwesterly to southeasterly winds converging over the region, a classic signature of enhanced monsoon flow. At upper levels (Figure 10(b)), wet years are characterized by positive anomalies, suggesting anticyclonic circulation and upper-level divergence, which supports deep convection. In contrast, dry years (Figure 10(c)) show positive anomalies over Zanzibar, reflecting a high-pressure system that suppresses convection through subsidence. At the upper level (Figure 10(d)), the GPH is lower (negative anomaly), and wind patterns show less divergence, indicating suppressed convection. The composite difference (Figure 10(e) and Figure 10(f)) reveals a robust dipole structure with strong negative anomalies at 850 hPa and positive anomalies at 250 hPa directly over Zanzibar, confirming that MAM rainfall variability is dynamically driven by vertically coupled circulation patterns.

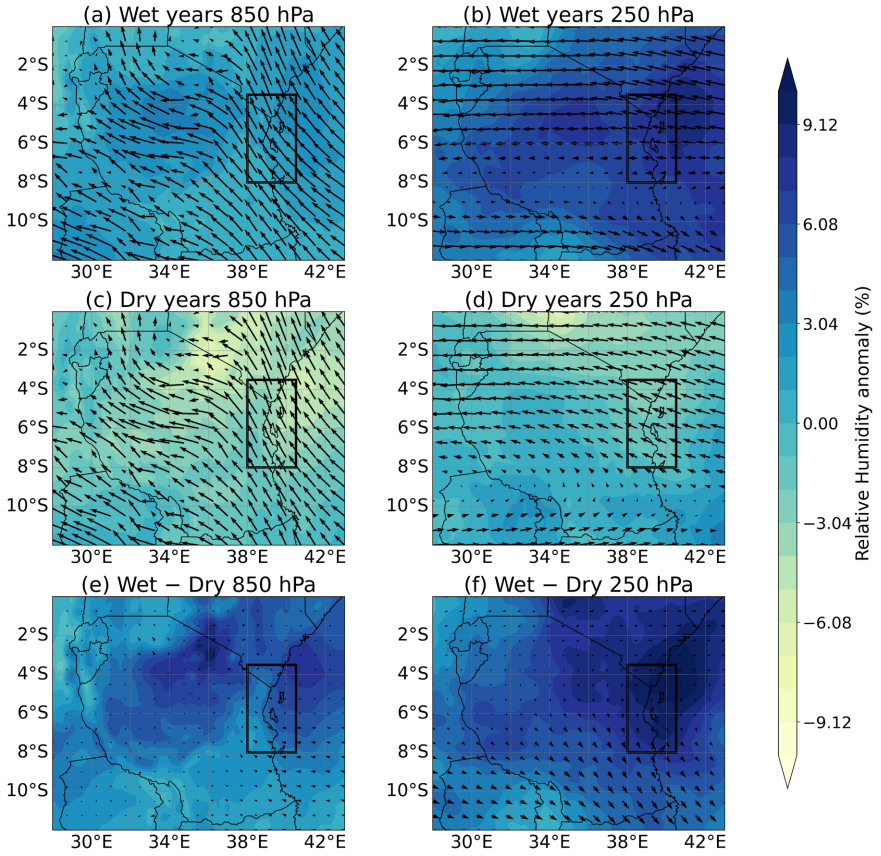

Figure 9. Composite MAM (March-April-May) 850 hPa and 250 hPa relative humidity (RH) anomalies and wind vectors for (a, b) wet years, (c, d) dry years, and (e, f) the wet–dry difference. Shading indicates RH anomalies, while black arrows represent wind direction and magnitude. The black box highlights the Zanzibar region (38˚E - 40.5˚E, 7˚S - 3.5˚S).

3.4.3. Composite Vertical Velocity (ω) across Pressure Levels during Wet and Dry Years

During the wet MAM seasons over Zanzibar (38˚E - 40.5˚E) shown by green line (**Figure 11(a)**), the atmosphere exhibits strong upward motion ($\omega < 0$) extending from the lower troposphere (~850 hPa) up to the upper troposphere (~200 hPa), with maximum ascent over Zanzibar. This deep, coherent rising motion is indicative of active convection and sustained rainfall, consistent with enhanced moisture convergence observed in the low-level wind fields. In contrast, during dry MAM years (**Figure 11(b)**), the vertical profile reveals dominant subsidence ($\omega > 0$) over the same longitude band, particularly between 700 - 400 hPa, suppressing cloud development and rainfall. The composite difference (**Figure 11(c)**) highlights a pronounced upward anomaly over Zanzibar, confirming that wet MAM seasons are characterized by stronger ascent and deep convection compared to dry seasons. These patterns align with the influence of moist easterly winds from the Indian Ocean, which converge over Zanzibar during MAM, and their modulation by ENSO-DMI concurrence revealed in section 3.3, where El Niño-pIOD or La Niña-pIOD phases have great chance to enhance or suppress convection, respectively.

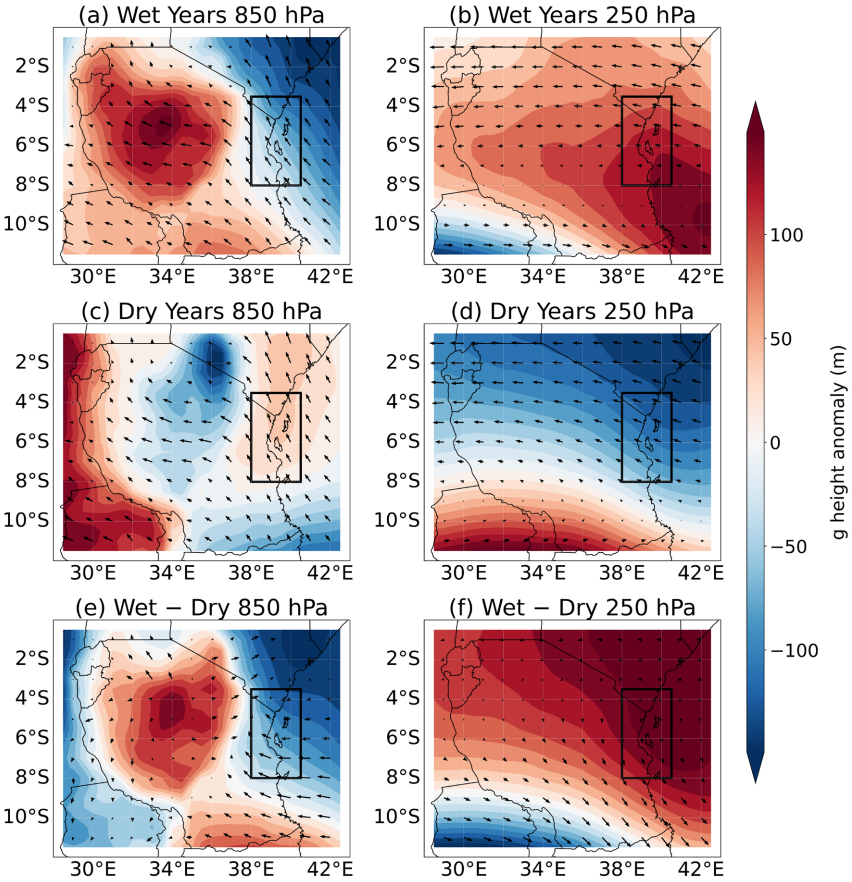

Figure 10. Composite MAM (March-April-May) geopotential height (GPH) anomalies (m) and wind vectors at (left column) 850 hPa and (right column) 250 hPa for (a, b) wet years, (c, d) dry years, and (e, f) Wet-Dry difference. Shading indicates GPH anomalies, while the black box highlights the Zanzibar region (38˚E - 40.5˚E, 7˚S - 3.5˚S).

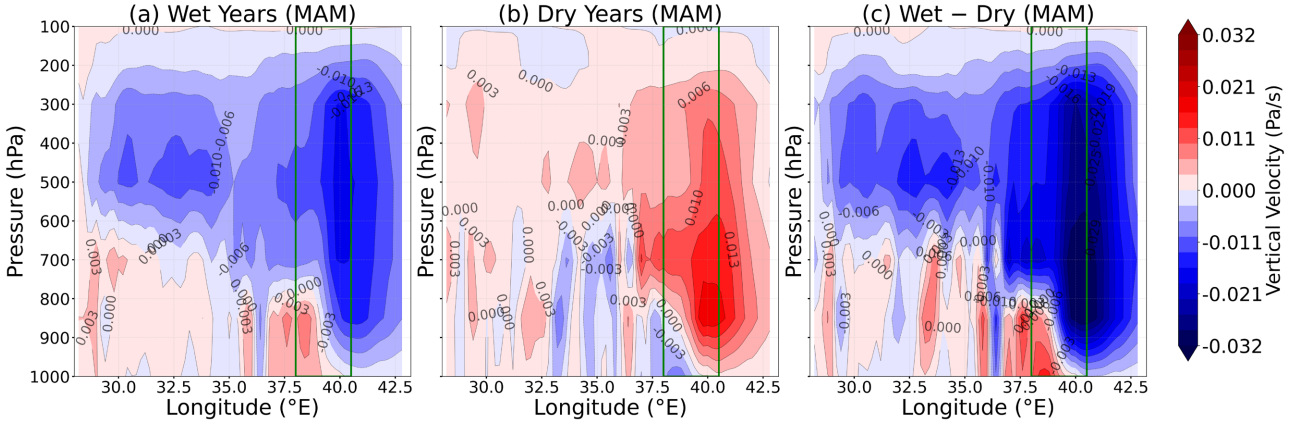

Figure 11. Vertical cross-sections of MAM (March-April-May) vertical velocity (ω, Pa/s) along 4˚S - 6˚S, averaged across latitudes, for (a) wet years, (b) dry years, and (c) Wet-Dry difference. Shading indicates ω values while contour labels show actual values. The green box highlights the Zanzibar region (38˚E - 40.5˚E).

3.4.4. Composite Anomaly of Moisture Flux Divergence (MFD) during Wet and Dry Years

The spatial composites of MFD anomalies and horizontal wind vectors over Zan-

zibar (black box) during wet and dry MAM seasons are shown in Figure 12. The results indicate that, the lower troposphere (Figure 12(a)) exhibits a pronounced convergence of moisture flux into the region, particularly from the Indian Ocean to the east and northeast, as indicated by the black vectors and positive moisture flux anomaly. This convergence is strongest within the black box encompassing Zanzibar, suggesting that moist air advection plays a dominant role in fueling rainfall. At upper levels (Figure 12(b)), wet years are characterized by outward moisture flux divergence, consistent with strong upper-level outflow supporting deep convection.

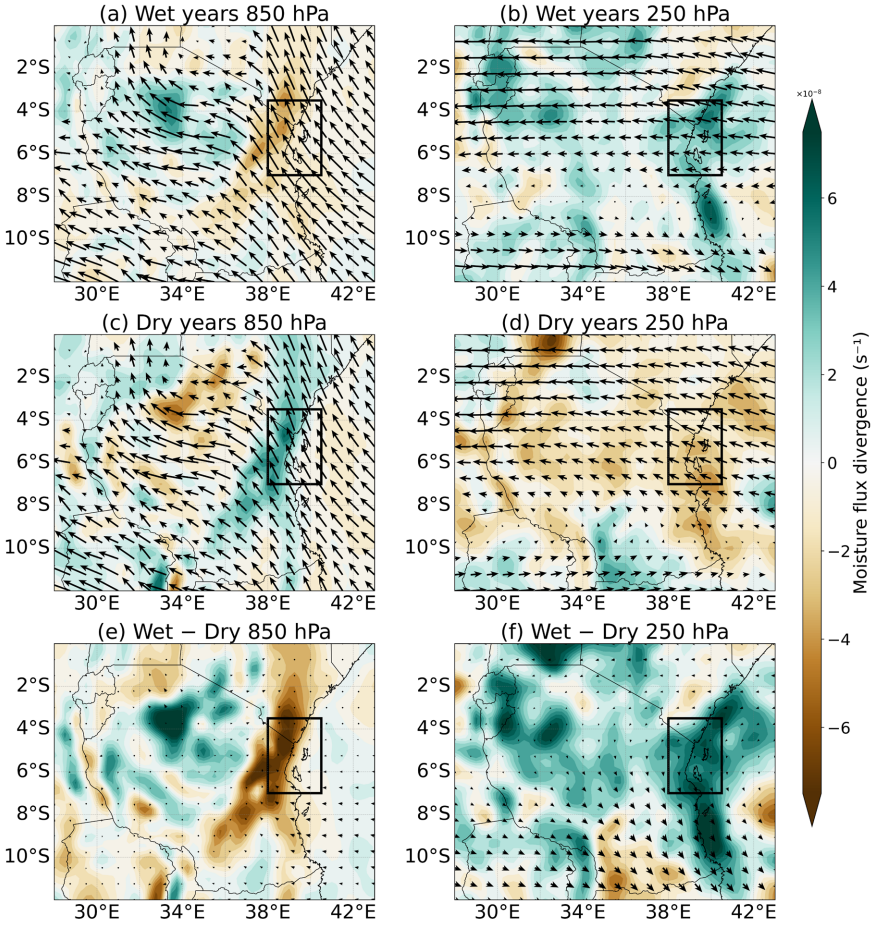

Figure 12. Composite MAM moisture flux divergence (MFD) anomalies (kg·m^{-2}·s^{-1}) and wind vectors at (a, d) wet years, (b, e) dry years, and (c, f) Wet-Dry difference, for (top row) 850 hPa and (bottom row) 250 hPa. The black box highlights the Zanzibar region (38˚E - 40.5˚E, 7˚S - 3.5˚S).

In contrast, dry MAM years (Figure 12(c)) show the divergent low-level moisture flux away from Zanzibar and inward upper-level moisture flux (Figure 12(d)), indicating suppressed convection and reduced vertical transport. The composite difference (Figure 12(e) and Figure 12(f)) highlights a robust dipole structure of enhanced moisture convergence at 850 hPa and divergence at 250 hPa directly over Zanzibar, confirming that rainfall variability is also dynamically

driven by vertically coupled moisture transport during wet and dry years.

4. Discussion

This study examined the concurrent impacts of ENSO and DMI on MAM rainfall variability in Zanzibar during the period 1981-2024. The EOF analysis revealed that EOF1, accounting for 88% of the total variance, represents a spatially coherent rainfall pattern across both Unguja and Pemba islands, indicating a regionally uniform response of MAM rainfall variability. The associated PC1 shows a strong positive correlation with SSTA in the Niño 3.4 region (r = 0.7) and a moderate positive correlation with the DMI (r = 0.3), highlighting the role of tropical Pacific and Indian Ocean variability in modulating Zanzibar's rainfall.

Further analysis of ENSO-DMI concurrence demonstrates that, in wet MAM season the concurrence of El Niño and positive IOD accounts for 50% of the wet years, whereas the concurrence of La Niña and positive IOD contributes 33.3% while El Niño and negative IOD co-occur by 16.7%. In contrast, dry years are largely dominated by La Niña conditions, with the concurrence of La Niña and positive IOD accounting for 71.5% of dry events, exceeding the contribution from La Niña with negative IOD or El Niño with negative IOD (28.5%). It should be noted that the frequency described here has some statistical limitations because of small sample sizes used in **Table 2**. Therefore, the percentages reflect the relative frequency of specific historical concurrent ENSO-IOD occurrences during the study period (1981-2024), rather than robust climatological probabilities. Also, the results indicate that El Niño-positive IOD combination exerts a stronger influence on MAM rainfall enhancement (wet years), while the La niña-positive IOD combination strongly influence reduction of MAM rainfall over the study domain. The combination of La niña-positive IOD during dry years highlights that, the above normal sea surface temperature in the western and southeastern Indian ocean does not guarantee enhancement of rainfall during MAM season in Zanzibar. In addition, some of the concurrent positive DMI signals observed during MAM may arise as a response to ENSO forcing through the atmospheric bridge or capacitor effect, rather than acting as fully independent drivers. ENSO likely plays a primary role in modulating large-scale circulation, with Indian Ocean SST anomalies reinforcing or modulating the rainfall response over Zanzibar.

Furthermore, while the IOD typically peaks during OND season (King'uza et al., 2025; Ntigwaza & Wang, 2024), the Indian Ocean Basin Mode (IOBM) and residual SST anomalies associated with the decay phase of ENSO may dominate during MAM (Guo et al., 2018). Hence, the observed SST gradients during MAM may not always represent a fully developed, locally coupled dipole event, but could reflect lagged or residual warming patterns linked to ENSO forcing. Overall, these findings collectively suggest that, when forecasting MAM rainfall over the study domain, meteorologists should pay attention to the combined influence of ENSO and DMI phases rather than considering a single mode alone. However, the rela-

tively weak long-term temporal correlation (r = 0.3) between PC1 and both ENSO and DMI indicates that additional atmospheric processes also play a substantial role in regulating MAM rainfall variability.

This inference is supported by the composite atmospheric circulation analysis. During wet/dry MAM years, the lower troposphere (850 hPa) is characterized by anomalous cyclonic/anticyclonic circulation and moisture convergence/divergence, while the upper troposphere (250 hPa) exhibits antagonistic circulation when compared to 850 hPa. The wet-dry composite anomalies relative to climatology indicate that enhanced rainfall is driven by anomalous low-level convergence and upward motion, whereas reduced rainfall is associated with low-level divergence and subsidence. Moreover, the results of the concurrent impacts of ENSO-DMI phases showed that La Niña conditions can override the influence of positive DMI anomalies during dry MAM seasons. This attribute can be explained in terms of Walker circulation. During dry MAM years (**Figure 11(b)**), the vertical profile reveals dominant subsidence ($\omega > 0$) over the same longitude band, particularly between 700 - 400 hPa, suppressing cloud development and rainfall. Therefore, enhanced Walker circulation during La Niña induces large-scale subsidence over the western Indian Ocean and East Africa, suppressing convection and vertical motion. This subsidence counteracts the low-level moisture convergence typically associated with positive Indian Ocean SST anomalies, thereby leading to reduced rainfall despite the presence of a positive DMI signal. These results are consistent with previous findings over Tanzania and Zanzibar (Chabaga et al., 2025; King'uza & Tilwebwa, 2019; Rwambo et al., 2025), underscoring the importance of regional atmospheric circulation in shaping rainfall variability with direct implications for agriculture, water resources, and livelihoods dependent on seasonal rainfall.

5. Conclusion

This study examined the concurrent impacts of the El Niño-Southern Oscillation and the Indian Ocean Dipole, represented by the Dipole Mode Index, during MAM rainfall variability in Zanzibar for the period 1981-2024. The major findings of the study are as follows.

1) The EOF analysis revealed that the leading mode of rainfall variability explains 88% of the total variance and exhibits a spatially coherent pattern across Unguja and Pemba islands, indicating a uniform regional rainfall response. The strong association between the leading principal component and SST anomalies in the Niño 3.4 region, together with a moderate relationship with the DMI, confirms the influence of large-scale ocean-atmosphere interactions on Zanzibar's seasonal rainfall.

2) The results further demonstrate that wet MAM seasons are most frequently modulated by the concurrent ENSO-DMI phases. While the El Niño-positive IOD combination exerts a stronger influence on MAM rainfall enhancement (wet years), the La niña-positive IOD combination strongly influence reduction of

MAM rainfall over the study domain, indicating that, above-normal sea surface temperatures in the western and eastern Indian Ocean do not necessarily lead to enhanced MAM rainfall in Zanzibar.

3) The wet-dry composite anomalies relative to climatology indicate that enhanced rainfall is driven by anomalous low-level convergence and upward motion, whereas reduced rainfall is associated with low-level divergence and subsidence.

Overall, this study underscores the necessity of considering multiple climate drivers simultaneously rather than in isolation. By highlighting the dominant concurrent ENSO-DMI phases and their relative frequencies, the research emphasizes the need for meteorological personnel to account for these interacting factors in seasonal rainfall forecasting in order to improve climate risk management and support evidence-based decision-making aimed at sustainable development and climate resilience in Zanzibar and similar coastal regions of East Africa.

Acknowledgements

The author gratefully acknowledges the Tanzania Meteorological Authority and the Ministry of Commerce of China (MOFCOM) for providing the opportunity to pursue this study. Sincere appreciation is extended to Prof. Zhao Yu for her supervision and invaluable guidance throughout the research. The author also acknowledges the European Centre for Medium-Range Weather Forecasts (ECMWF) for providing ERA5 data, the Climate Hazards Group for the CHIRPS precipitation dataset, and NOAA for the ERSST datasets.

Conflicts of Interest

The authors declare no conflicts of interest concerning the publication of this paper.

References

Abdalla, A. H., Kai, K. H., Khamis, S. A., Kondowe, A. L., Osima, S. E., King'uza, P. H. et al. (2023). The Influence of Climate Change and Variability on Spatio-Temporal Rainfall and Temperature Distribution in Zanzibar. *Atmospheric and Climate Sciences, 13,* 282-313. https://doi.org/10.4236/acs.2023.132016

Assenga, G. T., & Ndabagenga, D. M. (2025). Quasi-biweekly Oscillations and Midlatitude Wave-Train Modulation of Intraseasonal Temperature Variability over Tanzania during OND. *Discover Atmosphere, 3,* Article No. 39. https://doi.org/10.1007/s44292-025-00061-7

Assenga, G. T., Chabaga, C., Ndabagenga, D., & Mwageni, D. G. (2025). Intraseasonal Variability of 2020 Temperature over Tanzania during the October-November-December (OND) Season. *Atmospheric and Climate Sciences, 15,* 126-146. https://doi.org/10.4236/acs.2025.151006

Bakari, S. S., Suleiman, Z. N., Ali, H. R., & Kai, K. H. (2023). *Impacts of Pit latrines on Groundwater Quality in Squatter Settlements in Zanzibar.* https://doi.org/10.21203/rs.3.rs-2652203/v1

Borhara, K., Pokharel, B., Bean, B., Deng, L., & Wang, S. S. (2020). On Tanzania's Precipi-

tation Climatology, Variability, and Future Projection. *Climate, 8,* Article 34. https://doi.org/10.3390/cli8020034

Camberlin, P. (2018). *Climate of Eastern Africa.* Oxford Research Encyclopedia of Climate Science. https://doi.org/10.1093/acrefore/9780190228620.013.512

Chabaga, C. M., Asenga, G., & Ndabagenga, D. (2025). Intraseasonal Variability of Rainfall over Tanzania during March-April-May (MAM) Season of 2022. *Atmospheric and Climate Sciences, 15,* 218-247. https://doi.org/10.4236/acs.2025.151011

Dinku, T., Funk, C., Peterson, P., Maidment, R., Tadesse, T., Gadain, H. et al. (2018). Validation of the CHIRPS Satellite Rainfall Estimates over Eastern Africa. *Quarterly Journal of the Royal Meteorological Society, 144,* 292-312. https://doi.org/10.1002/qj.3244

Endris, H. S., Lennard, C., Hewitson, B., Dosio, A., Nikulin, G., & Artan, G. A. (2019). Future Changes in Rainfall Associated with ENSO, IOD and Changes in the Mean State over Eastern Africa. *Climate Dynamics, 52,* 2029-2053. https://doi.org/10.1007/s00382-018-4239-7

Finney, D., Msemo, H., & Marsham, J. (2021). Tanzania's 'forgotten' Cyclones and Concerns for the Future (pp. 1-5). https://www.preventionweb.net/news/tanzanias-forgotten-cyclones-and-concerns-future

Funk, C., Peterson, P., Landsfeld, M., Pedreros, D., Verdin, J., Shukla, S. et al. (2015). The Climate Hazards Infrared Precipitation with Stations—A New Environmental Record for Monitoring Extremes. *Scientific Data, 2,* Article No. 150066. https://doi.org/10.1038/sdata.2015.66

Greene, S., Pertaub, D., Mcivor, S., Beauchamp, E., & Sutz, P. (2020). *Understanding Local Climate Priorities Applying a Gender and Generation Focused Planning Tool in Mainland Tanzania and Zanzibar.* Issue Paper Produced by IIED's Climate Change Group. https://www.iied.org

Gudoshava, M., Nyinguro, P., Talib, J., Wainwright, C., Mwanthi, A., Hirons, L. et al. (2024). Drivers of Sub-Seasonal Extreme Rainfall and Their Representation in ECMWF Forecasts during the Eastern African March-To-May Seasons of 2018-2020. *Meteorological Applications, 31,* e70000. https://doi.org/10.1002/met.70000

Guo, F., Liu, Q., Yang, J., & Fan, L. (2018). Three Types of Indian Ocean Basin Modes. *Climate Dynamics, 51,* 4357-4370. https://doi.org/10.1007/s00382-017-3676-z

Hauke, J., & Kossowski, T. (2011). Comparison of Values of Pearson's and Spearman's Correlation Coefficients on the Same Sets of Data. *QUAGEO, 30,* 87-93. https://doi.org/10.2478/v10117-011-0021-1

Hersbach, H., Bell, B., Berrisford, P., Hirahara, S., Horányi, A., Muñoz-Sabater, J. et al. (2020). The ERA5 Global Reanalysis. *Quarterly Journal of the Royal Meteorological Society, 146,* 1999-2049. https://doi.org/10.1002/qj.3803

Intergovernmental Panel on Climate Change (IPCC) (2018). Summary for Policymakers. In *Global Warming of 1.5˚C: IPCC Special Report on Impacts of Global Warming of 1.5˚C above Pre-Industrial Levels in Context of Strengthening Response to Climate Change, Sustainable Development, and Efforts to Eradicate Poverty* (pp. 1-24). Cambridge University Press. https://www.cambridge.org/core/product/identifier/9781009157940%23prf2/type/book_part

Intergovernmental Panel on Climate Change (IPCC) (2023). Weather and Climate Extreme Events in a Changing Climate. In: *Climate Change 2021—The Physical Science Basis: Working Group I Contribution to the Sixth Assessment Report of the Intergov-*

ernmental Panel on Climate Change (pp. 1513-1766). Cambridge University Press. https://doi.org/10.1017/9781009157896.013

Kai, K. H., Ngwali, M. K., & Faki, M. M. (2021a). Assessment of the Impacts of Tropical Cyclone Fantala to Tanzania Coastal Line: Case Study of Zanzibar. *Atmospheric and Climate Sciences, 11,* 245-266. https://doi.org/10.4236/acs.2021.112015

Kai, K. H., Osima, S. E., Ismail, M. H., Waniha, P., & Omar, H. A. (2021b). Assessment of the Impacts of Tropical Cyclones Idai to the Western Coastal Area and Hinterlands of the South Western Indian Ocean. *Atmospheric and Climate Sciences, 11,* 812-840. https://doi.org/10.4236/acs.2021.114047

Kebacho, L. L. (2022). Interannual Variations of the Monthly Rainfall Anomalies over Tanzania from March to May and Their Associated Atmospheric Circulations Anomalies. *Natural Hazards, 112,* 163-186. https://doi.org/10.1007/s11069-021-05176-9

Kebacho, L. L., & Chen, H. (2022). The Dominant Modes of the Long Rains Interannual Variability over Tanzania and Their Oceanic Drivers. *International Journal of Climatology, 42,* 5273-5292. https://doi.org/10.1002/joc.7532

Kijazi, A., & Reason, C. (2009). Analysis of the 1998 to 2005 Drought over the Northeastern Highlands of Tanzania. *Climate Research, 38,* 209-223. https://doi.org/10.3354/cr00784

King'uza, P. H., Zhou, B., Okrah, A., Joan, B., & Limbu, P. (2025). Contribution of Very Heavy Rainfall Events to MAM and OND Rainy Seasons in Tanzania and Their Linkages to IOD and ENSO Events. *Theoretical and Applied Climatology, 156,* Article No. 580. https://doi.org/10.1007/s00704-025-05815-2

King'uza, P., & Tilwebwa, S. (2019). Inter-Annual Variability of March to May Rainfall over Tanzania and Its Association with Atmospheric Circulation Anomalies. *Geographica Pannonica, 23,* 147-161. https://doi.org/10.5937/gp23-22430

Mafuru, K. B., & Guirong, T. (2018). Assessing Prone Areas to Heavy Rainfall and the Impaction of the Upper Warm Temperature Anomaly during March-May Rainfall Season in Tanzania. *Advances in Meteorology, 2018,* Article ID: 8353296. https://doi.org/10.1155/2018/8353296

Magang, D. S., Ojara, M. A., Yunsheng, L., & King'uza, P. H. (2024). Future Climate Projection across Tanzania under CMIP6 with High-Resolution Regional Climate Model. *Scientific Reports, 14,* Article No. 12741. https://doi.org/10.1038/s41598-024-63495-w

Makula, E. K., & Zhou, B. (2021). Changes in March to May Rainfall over Tanzania during 1978-2017. *International Journal of Climatology, 41,* 5663-5675. https://doi.org/10.1002/joc.7146

Mbigi, D., & Xiao, Z. (2021). Tanzanian Rainfall Responses to El Niño and Positive Indian Ocean Dipole Events during 1951-2015. *Atmospheric and Oceanic Science Letters, 14,* Article ID: 100093. https://doi.org/10.1016/j.aosl.2021.100093

Ndabagenga, D. M., Yu, J., Mbawala, J. R., Ntigwaza, C. Y., & Juma, A. S. (2023). Climatic Indices' Analysis on Extreme Precipitation for Tanzania Synoptic Stations. *Journal of Geoscience and Environment Protection, 11,* 182-208. https://doi.org/10.4236/gep.2023.1112010

Nguyen-Le, D., Ngo-Duc, T., & Matsumoto, J. (2024). The Teleconnection of the Two Types of ENSO and Indian Ocean Dipole on Southeast Asian Autumn Rainfall Anomalies. *Climate Dynamics, 62,* 1-23. https://doi.org/10.1007/s00382-024-07163-9

Nicholson, S. E. (2017). Climate and Climatic Variability of Rainfall over Eastern Africa. *Reviews of Geophysics, 55,* 590-635. https://doi.org/10.1002/2016rg000544

Ntigwaza, C. Y., & Wang, W. (2024). Assessing the Relationship between October-November-December Rainfall and Indian Ocean Dipole in Recent Decades over Tanzania Fol-

lowing the 2011 Abrupt Change. *Journal of Geoscience and Environment Protection, 12,* 110-130. https://doi.org/10.4236/gep.2024.123007

Palmer, P. I., Wainwright, C. M., Dong, B., Maidment, R. I., Wheeler, K. G., Gedney, N. et al. (2023). Drivers and Impacts of Eastern African Rainfall Variability. *Nature Reviews Earth & Environment, 4,* 254-270. https://doi.org/10.1038/s43017-023-00397-x

Rwambo, I., Fan, Y., Yu, P., Chu, C., Nyasulu, M., & King'uza, P. (2025). Interannual Variability of Short Rains in Tanzania and the Influences from ENSO and the Indian Ocean Dipole. *Atmospheric and Oceanic Science Letters, 18,* Article ID: 100614. https://doi.org/10.1016/j.aosl.2025.100614

Sarkar, P. P., Sen, M. K., Kabir, G., & Hossain, N. U. I. (2024). Exploring Evolutionary Patterns in the Teleconnections between Indian Summer Monsoon Rainfall and Indian Ocean Dipole over Decades. *Climate Dynamics, 62,* 4041-4061. https://doi.org/10.1007/s00382-024-07116-2

Suleiman, R. A., Wen, W., Kazora, J., & Lipiki, E. J. (2023). Determination of October to December Seasonal Rainfall Variability, Its Seasonal Onset and Cessation Dates in Zanzibar, Tanzania. *Journal of Sustainability and Environmental Management, 2,* 179-189. https://doi.org/10.3126/josem.v2i3.59312

TMA (2022). *Statement on the Status of Tanzania Climate in 2022* (pp. 21, 1130).

TMA (2025). *Statement on the Status of Tanzania Climate in 2024 A 1 Statement on the Status of Tanzania Climate in 2021 Statement on the Status of Tanzania Climate in 2014 Tanzania Meteoro-Logical Authority (TMA) Statement on the Status of Tanzania Climate in 2024 Tanzania Meteorological Authority.*

WMO (2015). *Guidelines on the Definition and Monitoring of Extreme Weather and Climate Events.* WMO. https://library.wmo.int/viewer/58396/download?file=1310_Guidelines_on_DEWCE_en.pdf&type=pdf&navigator=1

Yu, J., & Kim, S. T. (2013). Identifying the Types of Major El Niño Events since 1870. *International Journal of Climatology, 33,* 2105-2112. https://doi.org/10.1002/joc.3575

Zhu, L., Meng, Z., Zhang, F., & Markowski, P. M. (2017). The Influence of Sea- and Land-Breeze Circulations on the Diurnal Variability in Precipitation over a Tropical Island. *Atmospheric Chemistry and Physics, 17,* 13213-13232. https://doi.org/10.5194/acp-17-13213-2017